Articles

Synthesis, Conformation, and Biological Characterization of a Sugar Derivative of Morphine that is a Potent, Long-Lasting, and Nontolerant Antinociceptive

Gemma Arsequell,[†] Mariona Salvatella,[†] Gregorio Valencia,*[,†] Alfonso Fernández-Mayoralas,[‡] Marco Fontanella,[§] Chiara Venturi,[§] Jesús Jiménez-Barbero,[§] Ezequiel Marrón,[||] and Raquel E. Rodríguez[||]

Unit of Glycoconjugate Chemistry, Instituto de Química Avanzada de Cataluña (IQAC−CSIC), Barcelona, Jordi Girona 18-26, E08034-Barcelona, Spain, Instituto de Química Orgánica General (IQOG), Juan de la Cierva 3, E28006-Madrid, Spain, Department of Protein Science, CIB−CSIC, Ramiro de Maeztu 9, E28040-Madrid, Spain, Instituto de Neurociencias de Castilla y León, University of Salamanca, Pintor Fernando Gallego 1, E37007-Salamanca, Spain

Received September 9, 2008

A synthetic mannoside derivative, namely, 6-morphinyl-α-D-mannopyranoside, shows a naloxone-reversible antinociception that is 100-fold more potent and twice as long lasting compared to morphine when administered intraperitoneally to rats in paw pressure and tail flick tests. The compound does not produce tolerance and binds to rat μ opioid receptors with twice the affinity of morphine. NMR studies suggest that differences of activity between the derivative and its parent compound M6G might be related to their differing molecular dynamic behavior.

Introduction

Chronic and acute pain is an unresolved medical problem, the prevailing treatment being the administration of morphine and its surrogates. Although the extensive use of morphine may suggest that it is the perfect analgesic drug, the side effects (i.e., constipation and respiratory depression) it shares with most opioids hamper its routine application outside the hospital.[1] In the search for alternative drugs, the important advances in the study of pain mechanisms driven by the new molecular biology tools have not provided substantial improvements. One of the factors in holding back drug development progress is the intrinsic nature of opioid receptors, which are integral, complex membrane-bound glycoproteins. No crystal structures of opioid receptors have been published, which limits receptor-based drug design techniques.[2] Accordingly, for the past 40 years, there has been little addition to the repertoire of drugs for treating severe chronic pain.[3] In spite of this, and using computational models of the opioid receptors, some progress has been made and new analogues, chemically modified natural opioid alkaloids, peptides, and nonpeptide, derivatives have been produced with limited therapeutic success.[4]

It is well established that, owing to the action of liver enzymes, 90% of a morphine dose administered in man is converted into a mixture of two glycoconjugates. By far the most abundant is the morphine-3-glucuronide (M3G[a]), accounting for 45−55% of the converted morphine, while a smaller proportion (10−15%) corresponds to morphine-6-glucuronide (M6G, **1**). For a long time, these were thought to be detoxifying inactive metabolites.[5] However, it has been found that while M3G is not endowed with analgesic properties, M6G (**1**) has pharmacological actions resembling those of morphine. When M6G is given systemically in animal models and humans, it shows fewer side effects and appears to be approximately twice as potent as morphine.[6] This suggests that systemic administration of M6G could provide benefits superior to similar doses of morphine.

The concept that M6G (**1**) can be a novel analgesic has slowly gained ground,[7] its superior side-effect profile[8] making it attractive to the pharmaceutical industry. The compound is currently under a phase III trial in a postoperative pain study.[9]

Further studies on M6G (**1**) have also proposed the existence of a specific receptor for this compound that corresponds to a splicing variant of the MOR1 gene.[8] Moreover, the idea that morphine is exclusively an exogenous opioid and that M6G is found only after morphine administration has also been challenged because mounting evidence suggests that both are produced in various vertebrate tissues. Thus, the discovery of an endogenous synthetic pathway for morphine[10,11] and the demonstration that M6G is present in adrenal chromaffin granules and secreted from chromaffin cells upon stimulation[12] indicate that there is a true endogenous morphinergic system.[13] This indicates that M6G (**1**) is not only a product of morphine catabolism but also a true neuroendocrine mediator possibly involved in many physiological systems.

In spite of these prospects, M6G (**1**) has hardly been explored with synthetic chemistry tools and the few structure−activity relationship studies[14] on M6G (**1**) have failed to identify more potent synthetic analogues. In the present paper, we provide experimental evidence that more potent M6G analogues can be found by, for instance, replacing the glucuronide part of the molecule by a mannose moiety (M6Man, **2**) (Figure 1).

Insight is also provided on how the structure and conformation of these molecules deduced by NMR spectroscopy and molecular modeling studies affect their biological activity. Thus, we

* To whom correspondence should be addressed. Phone: +34934006113. Fax: +34932045904. E-mail: gregorio.valencia@iqac.csic.es.
[†] Unit of Glycoconjugate Chemistry, Instituto de Química Avanzada de Cataluña (IQAC−CSIC).
[‡] Instituto de Química Orgánica General (IQOG−CSIC).
[§] Department of Protein Science, CIB−CSIC.
[||] Instituto de Neurociencias de Castilla y León, University of Salamanca.

[a] Abbreviations: M3G, morphine-3-*O*-β-glucuronide; M6G, morphine-6-*O*-β-glucuronide; M6Man; morphine-6-*O*-α-mannoside; BBB, blood−brain barrier; MPE, maximal possible effect.

10.1021/jm8011245 CCC: $40.75
Published on Web 04/07/2009

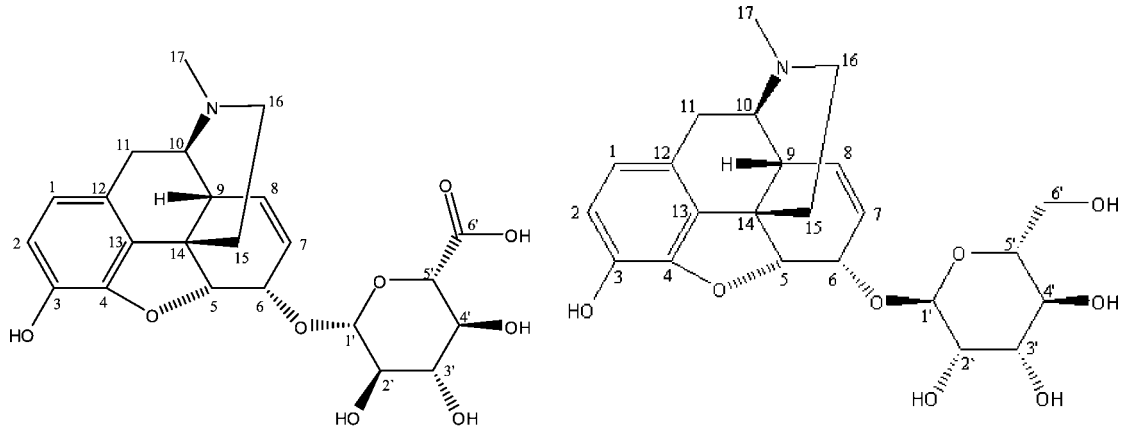

Figure 1. Chemical structure of M6Man (**2**) (right) as compared to natural M6G (**1**) (left).

disprove the hypothesis that M6G (**1**) shows two-sided behavior, adopting extended conformations in polar media and folded conformers in low polarity environments, which may allow the compound to cross membrane barriers such as the BBB.[15,16] Moreover, the enhanced potency of the mannoside with respect to M6G (**1**) seems to be related to the distinct dynamic behavior of these analogues.

Results and Discussion

The presence or absence of the glucuronide moiety is the exclusive structural difference between morphine and M6G (**1**). To better understand the contribution of the glucuronide part on the antinociceptive effect of M6G (**1**) and with the aim of finding new compounds with improved antinociceptive activity that mimic the structure of morphine-6-glucuronide (**1**), a drug discovery program was settled. The most significant finding was the identification of a mannoside derivative of morphine, namely, 6-morphinyl-α-D-mannopyranoside (M6Man, **2**) (Figure 1), with unusual antinociceptive activity when administered to rats. The first batches of the compound were prepared by boron trifluoride etherate catalysis[17] using peracetylated-α-D-mannose as a glycosyl donor, rendering 22% yield. However, silver triflate promotion and later the trichloroacetimidate method[18] raised the yields of further batches to 34 and 57%, respectively.

Antinociceptive Activity. The antinociceptive activity of the mannoside **2** was first evaluated by the tail flick[19] behavioural test using morphine sulfate as a reference. Compound **2** exhibited full antinociceptive action (100%) at a dose of 1 mg/kg, while the same dose of morphine only produced a 35% antinociceptive response. By further assaying lower amounts of the mannoside, the IC_{50} could be established at around 0.02 mg/kg, meaning that it is approximately 100-fold more potent than morphine. Another important feature of the morphine mannoside (**2**) is that its antinociceptive effect lasted for 5 h, which is twice the duration of that produced by morphine under the same conditions (Table 1).

Owing to these uncommon antinociceptive properties, a second set of antinociceptive tests, where the activity of the mannoside (**2**) was compared to both morphine and M6G (**1**), were conducted using the tail flick[19] and paw pressure[20] behavioural tests. This confirmed that the compound is 100-fold more active than and twice as long lasting as morphine (Figure 2). It is interesting to note that in this animal model of pain, M6G (**1**) is the less active compound. The antinociceptive activity of M6Man (**2**) could always be reversed by administration of 0.1 mg/kg of naloxone, implying that the analogue is acting through opioid receptors.

Table 1. Antinociceptive Activity of M6Man (**2**)[a]

compd	dose (ip) mg/kg)	animals	%MPE (%) 15 min	%MPE (%) 30 min	duration (h)
morphine sulfate	5	10	45	72	2.5
morphine-6-*O*-α-D-mannoside M6Man (**2**)	5	10	83	100	5
	1	10	56	100	5
	0.5	15	54	100	5
	0.2	10	57	100	5
	0.1	15	50	100	5
	0.05	20	56	84	5
	0.02	15	19	51	3.5
	0.01	15	−[b]	22	2
control (saline)		40	5	5	−
nontreated		30	3	4	−

[a] Sprague−Dawley male rats weighing 250−300 g have been used. Drugs were administered ip from saline solutions in 100−500 μL volumes. Antinociception was assessed by the tail flick test and expressed as %MPE after 15 and 30 min of the injection. The biological action of the compounds was reverted by a 5 mg/kg dose of ip naloxone. [b] -- means not determined.

Binding to Opioid Receptor Studies. Although the compound could possibly bind to κ and δ opioid receptors to confirm that M6Man (**2**) is a ligand for the μ opioid receptor, a competitive binding analysis was carried out using [^{3}H]-diprenorphine on HEK-293 cells stably expressing the rat μ opioid receptor. The affinity of the mannoside (**2**) for the receptor is two times higher than that of morphine (Figure 3).

Our experimental values for morphine affinity binding constants were close to the reference values of 2.5 ± 0.48 and 170 ± 6 nM for the high and low affinity sites, respectively.[21] Under similar conditions, literature values of M6G affinity are around an order of magnitude lower than that of morphine.[8]

Side Effect Studies. Because these remarkable antinociceptive properties could make this compound (**2**) a good candidate for a better analgesic drug, preliminary studies of its side effects were also carried out.

To compare the cardiovascular effects of the mannoside with those of morphine, equipotent antinociception doses should have been used. However, the closest equipotent doses for which antinociception has been checked were 1 mg/kg of the mannoside (100% antinociception after 30 min) and 5 mg/kg of morphine (70% antinociception). Using these doses, as shown

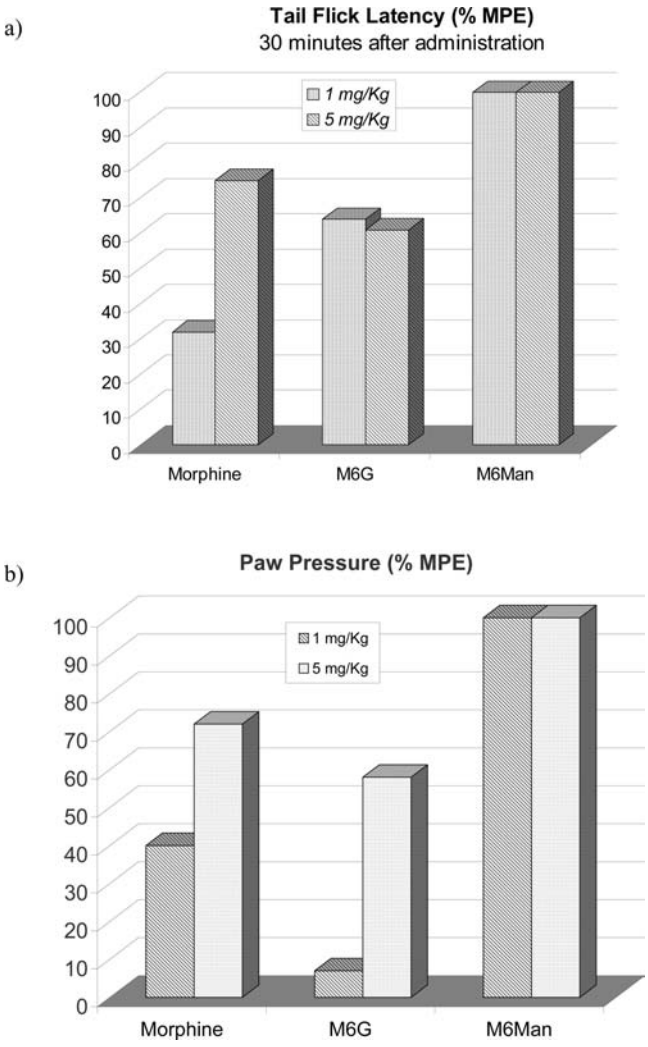

Figure 2. Antinociceptive effect of M6Man (**2**) as compared to morphine and M6G (**1**): (a) Tail flick, (b) paw pressure. Sprague−Dawley male rats weighing 250−300 g were used. Drugs were administered ip from saline solutions in 100−500 μL volumes. Values for antinociception given as %MPE are the mean of 12 animals.

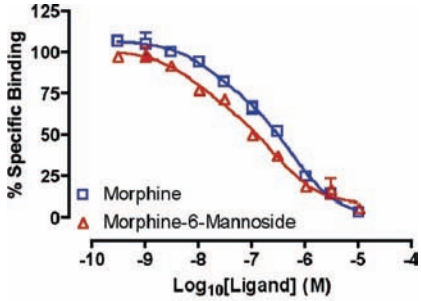

	Ki high (nM)	Ki low (nM)
Morphine	3.4 ± 0.7	113 ± 38
Morphine-6-mannoside	1.7 ± 0.5	55 ± 9.6

Figure 3. Competition binding analysis using [^{3}H]-diprenorphine (1.5 nM) and the unlabeled compounds morphine and M6Man (**2**) on HEK-293 cells stably expressing the rat μ opioid receptor. Nonspecific binding was determined as the binding in the presence of 10 μM naloxone. Results represent the mean ± SEM of three experiments performed in duplicate.

in Figure 4, morphine clearly produces a drastic depression of both arterial blood pressure and heart rate. Meanwhile, the mannoside, even at a much stronger antinociceptive dose (100% versus 70%), did not significantly affect the cardiovascular parameters as compared with a saline control dose.

In addition, the mannoside does not produce tolerance. A generally accepted method[22] consisting of a series of nine-day experiments were conducted at four different doses (5, 1, 0.1, and 0.05 mg/kg). As seen in Figure 5, the successive daily doses of the mannoside prompted the same antinociceptive responses throughout the nine-day period. Total antinociception (100%) could always be observed using the higher doses of 5, 1, and 0.1 mg/kg, and a steady response of around 55% was recorded for the very low 0.05 mg/kg dose. Tolerance is a well studied effect for morphine, and although new data continue to emerge[23] in this field, it is well established that under the experimental conditions used for the mannoside, a daily treatment with a standard dose of morphine (i.e., 7 mg/kg) may probably have triggered a stong tolerance effect by day 5, with antinociceptive values not significantly different from the baseline tail-flick latency on day 1.[24] The lack of tolerance of the mannoside was corroborated by using Alzet minipumps to ensure a continuous infusion and hence a constant blood concentration of the compound[25] (data not reported). Also, in this case, the antinociceptive effect remained constant throughout the time frame of the experiment. In addition, it is important to note that in the course of these experiments, significant metabolic changes such as loss of body weight were not observed.

Conformational Analysis. The unusual antinociceptive activity of the mannoside (**2**) shown after intraperitoneal administration can only be rationalized by assuming that it easily crosses the BBB. A similar explanation has also been hypothesized to explain the antinociceptive activity of M6G (**1**) after peripheral administration and the fact that when the BBB is bypassed and the compound is directly administered into the CNS, its activity is 13−800 times higher, depending on the assay.[26] In this case, no experimental evidence is available on how such a polar compound as M6G (**1**) can do so and only after computational studies has it been speculated that a conformational change facilitates its passive diffusion permeation throughout the BBB.[15,16] The chemical nature of such a conformational change would imply hindering the numerous polar groups of the molecule to make it more hydrophobic. To shed some light on this possibility and to check if a similar phenomena may take place with the mannoside (**2**), we have analyzed the solution conformation of both compounds in water and in a membrane-like environment.

Molecular Mechanics and Dynamics Calculations. The molecular mechanics calculations[27] were performed using the MM3* force field[28] as integrated in MACROMODEL.[29] The steric energy maps for **1** and **2** were computed as a function of the glycosidic (Φ) and aglyconic (Ψ) torsions.[30] According to the calculations, using the GB/SA solvent model for water, compound **1** presents two major minima, one extended conformation,[16] **A** (Φ = 42, Ψ = 147) with the typical *syn-exo*-anomeric geometry[31] for the Φ glycosidic torsion, and one folded conformation[16] **B**, the so-called anti-Φ minimum (Φ = 161, Ψ = 145). The population distribution according to a Boltzmann function from the energy values is 35% **A** and 65% **B**. In both cases, Ψ adopts a similar geometry, although fluctuations around the local and global minima do indeed take place. The corresponding views of these conformers are given in Figure 6.

In contrast, for the mannose derivative **2**, the MM3* analysis predicts the presence of a rather distinct distribution. Now, for this α-mannoside molecule (**2**), the calculations predict the existence of one very major conformation, with the typical *syn-*

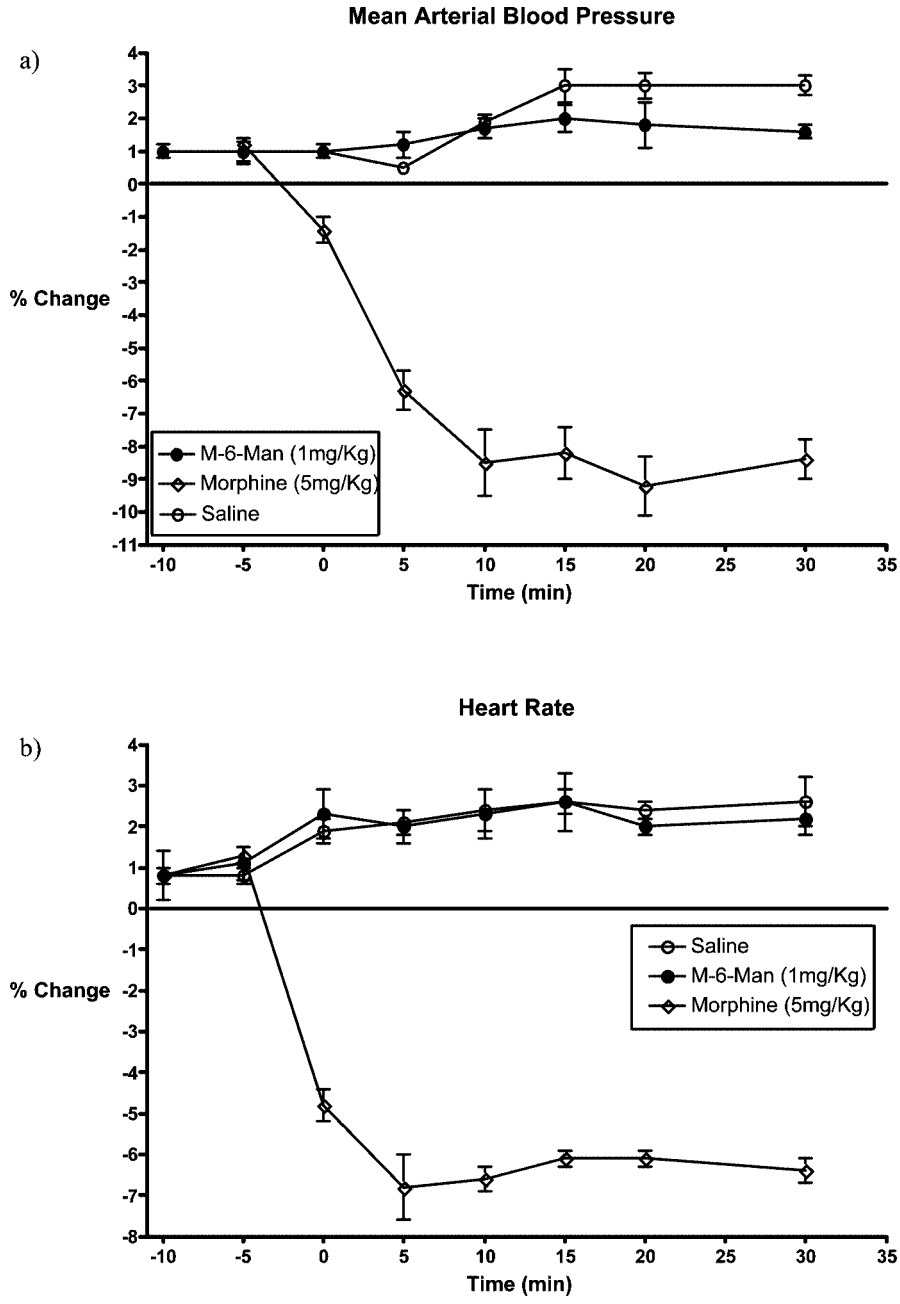

Figure 4. Cardiovascular effects of M6Man (**2**) as compared to an antinociceptive dose of morphine. (a) Blood pressure, (b) heart rate change. Doses: M6Man, 1 mg/kg, and morphine, 5 mg/kg ($n = 15$). Each point shown in the graphs represents the mean ± SEM of six different experiments for each saline, morphine, and M6Man.

exo-anomeric geometry[32] for the Φ glycosidic torsion (Φ = −73, Ψ = 103), as depicted in Figure 6 (bottom).

The low-energy conformations obtained in the MM3* calculations were used as input structures for MD simulations to verify the conformational space available for the different minima. These simulations were performed during 7 ns also using the same force field. The conformational behavior of Φ and Ψ torsions were monitored during the simulation time and all the minima found in the MM calculations were shown to be conformationally stable (see the Supporting Information).

Indeed, for **1**, the MD results are in good agreement with those predicted by MM, independently of the starting structure. The simulations predict that the glycosidic torsion oscillates between the *exo-syn* and the *anti* conformations, whereas for the Ψ aglyconic torsion, there are clear oscillations around the global minimum geometry of 145°. For **2**, only one conformer is observed in terms of Φ, while oscillations of around one single minimum also take place for Ψ, as described above for **1**.

NMR Spectroscopy. The validity of the theoretical results was verified through NMR spectroscopy to assess the final conformational distribution for **1** and **2**. The chemical shifts in water, at 298 K, are listed in Table 2. The assignment of the resonances was made using a combination of COSY, TOCSY, NOESY, HSQC, HMBC, and HSQC-TOCSY experiments (see figures in the Supporting Information).

For the M6G derivative **1**, duplication of the NMR signals corresponding to the C14−C17 region was evident in the TOCSY, HSQC, and NOESY experiments. Indeed, in the NOESY experiments, exchange cross peaks (with the same sign as the diagonal peaks) were observed. This fact indicates that a dynamic process is taking place around the C14−C17 region, which has probably to do with the well-known nitrogen

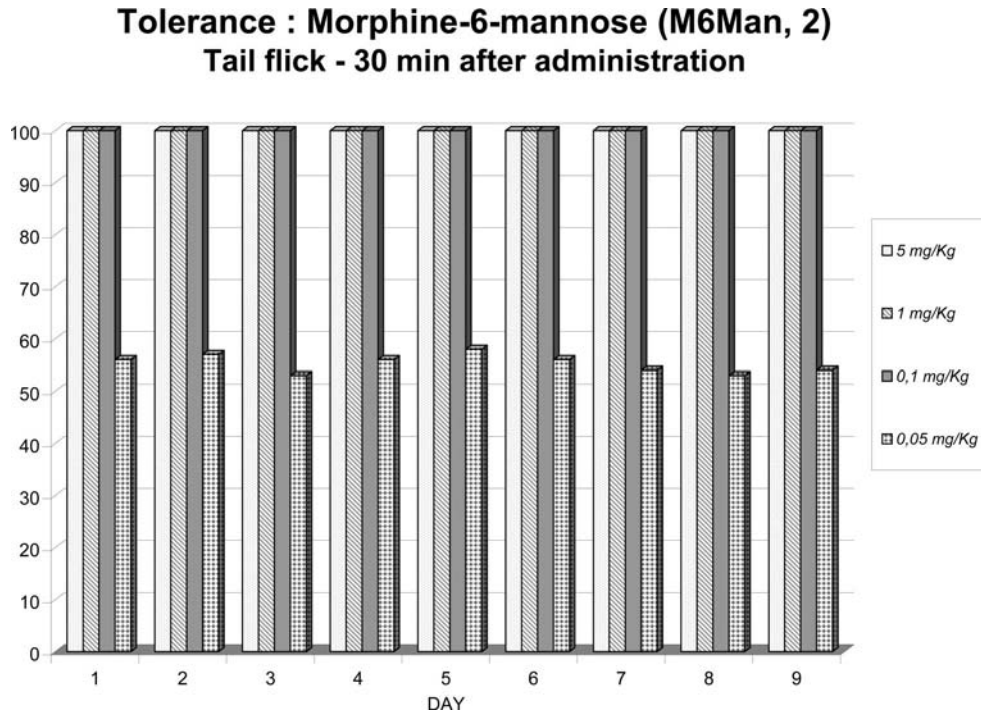

Figure 5. Tolerance effects. Tail flick response after consecutive daily injections of different doses of M6Man **2** (0.05, 0.1, 1, and 5 mg/kg). Sprague−Dawley male rats weighing 250−300 g were used. Drugs were administered ip from saline solutions in 100−500 μL volumes. Antinociception is expressed as the mean value of %MPE of groups of 10 animals.

inversion process. Nevertheless, this phenomenon does not take place for the M6Man analogue, **2**.

The conformation of the morphine ring is well-known[33] and will not be described here, although it should be mentioned that the NOE and coupling values agree perfectly with the described structure (Tables 3 and 4).

The global shapes of these molecules are given by the relative orientation of the morphine and the sugar moieties, resulting in the conformations around the glycosidic linkages, which are defined by the torsion angles Φ and Ψ. Regarding the sugar moieties, the *J* values[34] for the ring protons indicate that the pyranose rings of both **1** and **2** adopt the usual $^4C_1$ chair conformation (Table 2). The intermediate values observed for the C5′−C6′ lateral chain of **2** are in agreement with the well-described equilibrium between the gg:gt conformers[35] for a mannopyranose ring.

For **1** and **2,** no homonuclear *J* couplings are available around the Φ,Ψ glycosidic linkages, and thus the conformational distribution has to be derived from the NOE information,[36] assisted by the calculations described above. The most relevant key NOE information is gathered in Table 4.

The intensities of the observed NOEs were transformed into distances, using a full matrix relaxation approach[35] and compared to those estimated by the molecular mechanics and dynamics calculations.[36]

The key NOEs for the conformational information around Φ,Ψ are those involving the sugar anomeric protons GlcA H-1′ for **1** (Man H-1′ for **2**) and the proximal protons of the morphine moiety. In all cases, NOEs were positive; that is, they showed different signs from the diagonal peaks. When comparing the NOEs calculated distances (full matrix relaxation approach) for compound **1** with those obtained from MM3* calculations of low energy structures, it can be deduced that only the *syn* conformer may explain the observed NOEs. The observed NOEs for the *anti* (folded[16]) conformer are indeed far from those expected. Nevertheless, the best fit between observed and predicted NOE data (table in the Supporting Information) was obtained when local motion around the extended *syn*-conformer was considered.[37] Thus, different effective correlation times were seen for the intrasugar cross peaks and for the sugar−morphine cross peaks. This is a clear indication of the internal flexibility of M6G, with distinct motion in the different parts of the molecule. Indeed, when the NOEs of the sugar ring were adjusted, using 220 ps as correlation time, the sugar−morphine and intramorphine NOEs appear overestimated. In contrast, when the correlation time was set to 270 ps, a good fitting between expected and simulated sugar−morphine NOEs could be recorded for all the conformers located in the MD simulation around the *exo*-anomeric *syn* Φ geometry.

For compound **2**, a comparison of similar MM3* calculations with experimental NOE data suggests that this compound is also exclusively populating the *exo* Φ geometry. Again, the best fit was obtained by considering the conformers found in the MD simulation around the global minimum geometry and, in this case, the difference between the effective correlation times for the intrasugar cross peaks (280 ps) and for the sugar−morphine interresidual cross peaks (300 ps) was fairly small.

The conformation of these molecules was also studied in a membrane-like environment, using deuterated SDS micelles. The experiments were conducted at a concentration of ligand ca. 2 mM and SDS 40 mM in D_2O, thus at a 1/20 molar ratio. No significant changes in the coupling constants of the morphine or sugar moieties were observed for either compound when compared to their values in water solution. The recorded NOEs in the NOESY spectra were negative, that is, showing the same sign of the diagonal peaks, and thus indicating that the average rotational correlation is much larger than that described above for the experiments in water solution, where the NOEs were positive. This is an indication that both **1** and **2** interact with the SDS micelles.

As in the case of the experiments in water, in SDS micelles, all the experimental NOEs and deduced distances for both

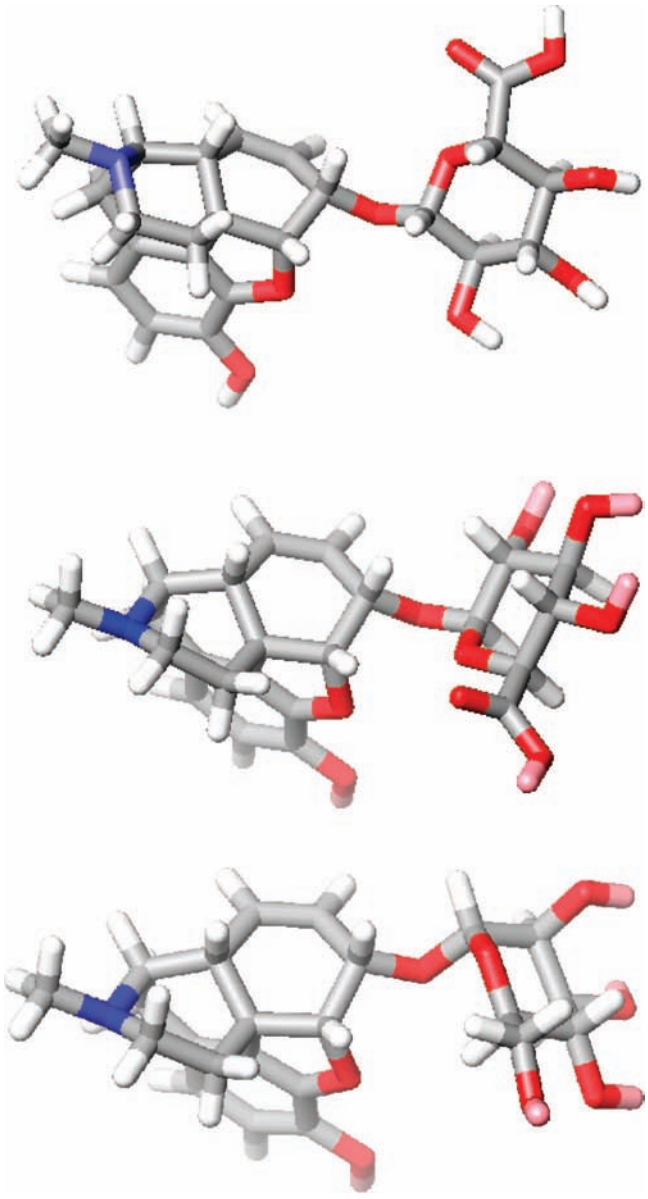

Figure 6. The major conformers of compounds **1** and **2**. From top to bottom, the extended (Φ *syn-exo*-anomeric) conformation of M6G, the folded anti-Φ conformer of M6G. The bottom figure represents the only Φ *syn-exo*-anomeric conformer of M6Man.

molecules point toward the existence of a very major *syn*-conformer around the glycosidic linkages. In addition, internal motions around the glycosidic linkages of **1** were also detected because different average correlation times were required to fit the NOEs for the morphine moiety (970 ps) and the sugar ring (740 ps). For **2**, the required correlation times to fit both sugar and morphine entities were basically the same, 770−780 ms.

In conclusion, the conformational behavior for M6G (**1**) and its mannosyl analogue M6Man (**2**) in water solution or in SDS micelles is relatively similar in terms of the contributing conformations. The integrated information deduced for the coupling constants and NOEs and the assistance of the geometries calculated by molecular mechanics[38] show that there is a major *exo*-anomeric extended[16] conformation around the Φ angle of both molecules with local motion around the global minimum geometry. No contribution of other conformers around the glycosidic linkage is observed in water solution, thus supporting former predictions arising from theoretical calculations.[16,27] The MM3* calculations for M6G only provide a qualitative description of the actual population distribution because they predict a high percentage of the folded *anti*-Φ conformer.[39] On top of these features for the glycosidic linkage, only the M6G analogue displays additional conformational dynamics around the C14−C17 morphine region.

Table 2. Chemical Shifts (δ, ppm) and Coupling Constants (*J*, Hz) for the Key Protons of M6G (**1**) and M6Man (**2**) (ca. 5 mM) at 500 MHz in Water Solution and 298 K[a]

proton	M6G δ (ppm)	M6G *J* (Hz)	proton	M6Man δ (ppm)	M6Man *J* (Hz)
		Morphine Moiety			
M H1	6.73	6.6		6.77	6.2
M H2	6.65	6.6		6.69	6.2
M H5	5.15	5.0		5.26	5.6
M H6	4.45	5.0, 2.7		4.57	5.6, 2.5
M H7	5.80	9.7		5.85	9.9
M H8	5.46	9.7		5.39	9.9, 2.2
M H9	2.93			2.94	
M H10	3.99			4.21	
M H11	3.20			3.29	
M H11′	2.78	6.8		2.90	5.6
M H15	2.27	14.2, 6.5		2.32	13.7
M H15′	2.05	14.2		2.16	13.7
M H16	3.12			3.37	13.4
M H16′	2.94	13.3, 6.1		3.09	
M H17	2.82			2.99	
		Sugar Moiety			
GlcA H1′	4.73	7.8	Man H1′	5.06	2.1
GlcA H2′	3.40	8.4, 7.8	Man H2′	4.03	3.3, 2.1
GlcA H3′	3.58	9.3, 8.4	Man H3′	4.00	3.3, 9.9
GlcA H4′	3.52	9.3, 9.3	Man H4′	3.68	9.9, 9.9
GlcA H5′	3.74	9.3	Man H5′	3.95	9.9, 2.2, 6.6
			ManH6′a	3.92	2.2, 12.4
			ManH6′b	3.80	6.6, 12.4

[a] The sugar protons are primed. The values in SDS micelles (40 mM in D_2O) are basically identical.

Because of the different chemical nature of the two glycosidic linkages of **1** (β-GlcA) and **2** (α-Man), the relative orientation of the sugar and the morphine moieties is rather different, as can be observed in the superimpositions (Figure 7).

However, the quantitative analysis of the NOE intensities at a variety of mixing times under two different experimental conditions (water or SDS micelles) indicates that the rate of motion around the glycosidic linkages of **1** and **2** is rather different and this fact was not foreseen a priori. Also, the obtained data indicate that the polarity of the medium does not influence the presentation of the polar groups of these molecules. Thus, although merely speculative, the different potency of **1** versus **2** might be related to their different conformational preferences, the different dynamic behavior, or simply to a proper requirement of polar and apolar surfaces of **1** and **2** to establish key interactions with their environment.

The quest for a model of their complexes with the proper receptors should answer some of the questions raised here.

Conclusions

In conclusion, the present report provides the first example of a synthetic morphine glycoside derivative, namely, 6-morphinyl-α-D-mannopyranoside (M6Man, **2**), that mimics the natural morphine metabolite M6G. When administered intraperitoneally at equal doses, the antinociceptive action of the compound is 100-fold higher than and twice as long lasting as morphine when examined in rats using paw pressure and tail flick tests. This antinociceptive effect is always reversed by naloxone (0.1 mg/kg). Receptor binding selectivity was not fully examined, however, the mannoside **2** is a μ opioid receptor

Table 3. Selected Experimental Coupling Constant Values for Compounds M6G (**1**) and M6Man (**2**) at 500 MHz in Water Solution and 298 K[a]

proton pair	experiment for **1**, J_{exp} (water)	*syn*-Φ conformer (extended), J_{theor}	*anti*-Φ conformer (folded), J_{theor}	experiment for 2, J_{exp}	*syn*-Φ conformer (extended), J_{theor}
			Morphine Moiety		
$J_{1,2}$	6.6	6.3	6.2	6.2	6.2
$J_{10,11'}$	6.8	6.5	5.7	5.7	5.8
$J_{8,9}$	3.0	3.0	2.6	2.3	2.7
$J_{6,7}$	2.8	2.8	2.6	2.5	2.6
$J_{5,6}$	5.0	4.8	6.1	5.7	5.7
$J_{15,16}$	6.5	6.9	6.8	5.0	5.4
			Sugar Moiety		
$J_{1',2'}$	7.9	8.0	7.8	2.1	2.4
$J_{2',3'}$	8.5	9.2	8.9	3.4	3.1
$J_{4',5'}$	9.9	10.1	10.1	9.9	9.7

[a] The values in SDS micelles (40 mM in D_2O) are basically identical. The comparison with the basic conformers calculated by MM3* calculations is also given. The agreement between the experimental and theoretical values is excellent. The sugar protons are primed. Coupling values cannot be used to discriminate between the folded and extended conformers of **1**.

Table 4. Estimated Distances from the NOE Cross Relaxation Rates for Selected Proton Pairs of M6G (**1**) and Ma6Man (**2**)[a]

proton pair	NOE-based distance (Å) for **1**	*syn*-Φ extended conformer	*anti*-Φ folded conformer	proton pair	NOE-based distance (Å) for 2	syn-Φ extended conformer
GlcA H1′−GlcA H5′	2.4	2.4	2.4	Man H1′−Man H 5′	not detected	3.7
GlcA H1′−GlcA H2′	3.0	3.1	3.1	Man H1′−Man H2′	2.5	2.5
GlcA H1′−M H6	2.5	2.5	3.6	Man H1′−M H6	2.3	2.4
GlcA H1′−M H5	2.8	2.8	4.2	Man H1′−M H5	not detected	4.3
GlcA H1′−M H7	3.9	3.8	4.4	Man H1′−M H7	2.8	3
GlcA H2′−M H6	4.0	4.0	2.2	Man H2′−M H6	not detected	4.4
MH 7−MH 8	2.5	2.5	2.4	MH 7−MH 8	2.5	2.5
MH 7−MH 6	2.8	2.8	2.8	MH 7−MH 6	2.8	2.9
MH 6−MH 5	2.35	2.35	2.35	MH 6−MH 5	2.35	2.35

[a] Intrapyranose ring (with the GlcA H 1′−GlcA H 5′ or Man H1′−Man H2′ contacts taken as reference, 2.4 Å), intramorphine (with the H5−H6 contact taken as reference, 2.35 Å), and inter-residue (sugar−morphine) contacts are given. The sugar protons are primed. The data were acquired at 500 MHz in water solution or in 40 mM SDS micelles in water (same average experimental distances within experimental error) and 298 K. The agreement with only the presence of the *syn*-Φ conformers of both **1** and **2** is excellent.

ligand with twice the affinity of morphine. In addition, in this same animal model, the compound does not produce tolerance and does not affect cardiovascular parameters such as heart rate and arterial blood pressure. Solution conformation studies by NMR and molecular mechanics and dynamics calculations of both M6Man and M6G indicate that their distinct molecular dynamic behavior rather than their conformation may be responsible for their activity differences. In addition, NMR experimental evidence could not confirm the accepted hypothesis that M6G is able to show a less polar folded conformation that may facilitate the BBB penetration of the compound.

Experimental Section

Chemical Synthesis. General Methods. All reagents were purchased from Sigma-Aldrich, Fluka, or as otherwise stated. Samples of M6G and morphine were obtained respectively from Ultrafine (UFC, Manchester, UK) and Alcaliber S.A. (Madrid, Spain) with the permission of Agencia Española de Medicamentos y Productos Sanitarios, Area de Estupefacientes. [^{3}H]-diprenorphine was from Perkin-Elmer. Commercial chemicals were always used without purification. Dry solvents were prepared using standard procedures, according to Vogel's manuals, with distillation prior to use. All new compounds were characterized by ^{1}H NMR, ^{13}C NMR, and reverse phase HPLC, in addition to MALDI-TOF mass spectroscopy and HR-MS. All spectral data reported here were obtained from the acetate salt form of the products. Melting points were obtained with a Fisher Scientific micro melting point apparatus and were uncorrected. NMR experiments were recorded on a Bruker Avance 500 instrument at 25 °C. Chemical shifts were referenced to external DSS in D_2O. One-dimensional spectra were acquired using 32K data points, which were zero-filled to 64K data points prior to Fourier transformation. Absolute value COSY and HMBC and phase-sensitive HSQC and HSQC-TOCSY spectra as well as NOESY experiments (mixing times of 300, 400, and 700 ms) were acquired using standard techniques. Acquisition data matrices were defined by 2K × 256 points, multiplied by appropriate window functions and zero-filled to 2K × 512 matrices prior to Fourier transformation. Baseline correction was applied in both dimensions. Spectra were processed using the Bruker XWIN-NMR program on a personal computer. TLC analyses were carried out on Merck Kieselgel 60 F_{254} silica gel plates. Visualization was by UV light (254 nm). Purifications by column chromatography were carried out using Silica Gel 60 (70−200 μm) from SDS and solvents for synthesis of GPR grade. Yields were not maximized. The final target compound purity was tested by HPLC, and a satisfying purity of >95% was achieved using the described purification method. Reverse-phase HPLC analyses were performed on a MERCK-HITACHI (D-6000) HPLC system with an UV L-4000 detector (λ = 214 nm), a L-6200 pump, and an AS-2000 automatic injector, using a Merck LiChroCART 250-4 LiChrospher 100-5 RP-C18 column (250 mm × 4.6 mm) with injection volume at 10 μL and sample concentrations at 1−2 mg/0.5 mL in 100% water; the sample was detected at single wavelength of 214 nm with a mobile phase system composed with a mixture of acetonitrile:water each containing an 0.1% of TFA at 1 mL/min flow. The column was maintained at room temperature. MS (ESI) data was obtained in a mass spectrometer from Micromass, UK and MALDI-TOF-MS in a VOYAGER-DE-RP (Applied Biosystems, Framingham, MA). The MALDI-TOF mass spectrometer was equipped with a nitrogen laser (337 nm) and operated in positive ion mode. HRMS spectra (UPLC-TOF/MS) were recorded on a Waters ACQUITY UPLC system with a Waters LCT Premier XE mass spectrometer operating in the positive ion electrospray mode. Water and acetonitrile were used as carrier solvents.

General Procedure 1. Under argon atmosphere, 5 equiv of boron trifluoride ethyl etherate complex ($BF_3 \cdot Et_2O$) was added dropwise to a solution of 1.1 equiv of 3-*O*-acetyl morphine and 1 equiv of

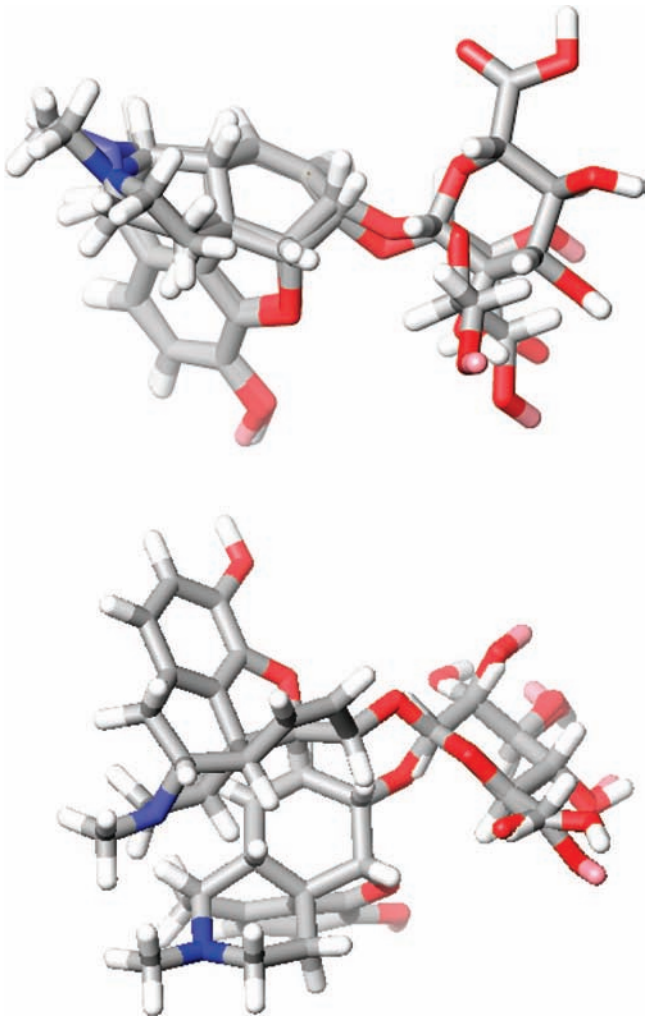

Figure 7. Superimposition of the major extended conformers of compounds M6G (**1**) and M6Man (**2**), as deduced from the experimental NMR data. Top: the morphine moieties are superimposed: different spatial orientations of the polar hydroxyl groups of the sugar take place. Bottom: the sugar rings are superimposed: different spatial orientations of the morphine fragment take place.

1,2,3,4,6-penta-*O*-acetyl-α-D-mannopyranose in dry methylene chloride. The resulting mixture was stirred at 0 °C for 30 min and then kept overnight at room temperature. The reaction mixture was diluted with methylene chloride and partitioned between water and CH_2Cl_2. The water layer was extracted with CH_2Cl_2. The combined CH_2Cl_2 solution was washed with H_2O, brine, and dried with Na_2SO_4. After concentration, the residue was purified by silica gel column with a $CHCl_3$/MeOH gradient mixture from (100:0) to (8:2) solvent system as eluent to give the pure peracetylated morphine glycoconjugate. Deacetylation step: a solution of 0.19 equiv of the peracetylated 6-(3-*O*-acetyl)-morphinyl-α-D-mannopyranoside in 8 mL of 0.1 M sodium methoxide in methanol was stirred at room temperature. After 60 min, the reaction mixture was neutralized with acetic acid and the solvent removed under vacuum. The crude residue was purified on a silica gel column eluted with an isocratic solvent mixture of ethyl acetate/water/methanol (3:2:1). Solvent evaporation and further lyophilization of the pure fractions from an aqueous acetic acid solution afforded 106 mg (22% overall yield) of the title compound as a white solid.

General Procedure 2 (Köenigs−Knorr Method). To a solution of 1.5 equiv of 3-*O*-acetyl morphine and 1 equiv of 1-bromo-2,3,4,6-tetra-*O*-acetylmannopyranose in dry methylene chloride at 0 °C, 1.3 equiv of silver triflate was added. The reaction mixture was stirred under an argon atmosphere. After 3 h, dry pyridine was added and the reaction was left to proceed a further 24 h. The dark crude mixture was filtered through celite, and the solvent was evaporated. The residue was purified as above, yielding the protected morphine glycoside. After a deacetylation and purification step as in procedure 1, the mannoside was obtained in 34% overall yield.

General Procedure 3 (Trichloroacetimidate Method). In a round-bottom flask, a solution of 1.34 equiv of 3-*O*-acetyl morphine and 1 equiv of 1-trichloroacetimidate-2,3,4,6-tetra-*O*-acetyl-mannopyranose was prepared in dry methylene chloride. The mixture was stirred under an argon atmosphere at 0 °C until the addition of 5 equiv of the $BF_3 \cdot Et_2O$ complex. After 22 h of reaction at room temperature, the mixture was diluted with methylene chloride, washed with 5% sodium bicarbonate, purified, and deacetylated as in procedure 1, yielding the morphine mannoside **2** in a 57% overall yield.

(5α,6α)-7,8-Didehydro-4,5-epoxy-3-hydroxy-17-methylmorphinan-6-yl-α-D-mannopyranoside (2) [Morphinyl-6α-D-mannopyranoside acetate (2)]. Compound **2** was prepared by following the general procedures 1, 2, and 3 in 22%, 34%, and 57% overall yield, respectively. $[\alpha]^{20}_D$ −47.05 (c = 1, MeOH); mp 170−175 °C. ^{1}H NMR data (500 MHz, Bruker Avance spectrometer, D_2O as solvent, DSS as internal standard and 298 K): δ 6.77 (*J* 6.2 Hz, H-1), 6.69 (*J* 6.2 Hz, H-2), 5.85 (*J* 9.9 Hz, H-7), 5.39 (*J* 2.2 Hz, H-8), 5.26 (*J* 5.6 Hz, H-5), 5.06 (*J* 2.1 Hz, H-1 Man), 4.57 (*J* 2.5 Hz, H-6), 4.21 (H-10), 4.03 (*J* 3.3 Hz, H-2 Man), 4.00 (*J* 9.9 Hz, H-3 Man), 3.95 (*J* 2.2 Hz, *J* 6.6 Hz, H-5 Man), 3.92 (*J* 2.2 Hz, *J* 12.4 Hz, H-6a Man), 3.80 (*J* 12.4 Hz, *J* 6.6 Hz, H-6b Man), 3.68 (*J* 9.9 Hz, H-4 Man), 3.37 (*J* 13.4 Hz, H-16), 3.29 (H-11), 3.09 (*J* 13.3 Hz, *J* 6.1 Hz, H-16′), 2.99 (H-17), 2.94 (H-9), 2.90 (*J* 5.6 Hz, H-11′), 2.32 (*J* 13.7 Hz, *J* 6.5 Hz, H-15), 2.16 (*J* 13.7 Hz, H-15′). ^{13}C-NMR (50 MHz, CD_3OD): δ 178 (C3), 147,7 (C4), 140,2 (C7), 134.9 (C═O), 132.1, 130.8 (C11), 128.6 (C12), 124.8 (C8), 120.5 (C1), 118.3 (C2), 102.3 (C1′β), 92.4 (C5), 92.1, 75.0 (C5′), 74.7 (C3′), 72.4 (C2′), 72.3 (C4′), 68.8 (C6′), 63.2 (C6), 61.1 (C13), 44.2 (C16), 42.0 (C17), 40.1 (C9), 34.7 (C14), 23.1 (Ac), 22.6 (C10). (ESI) *m*/*z*: 448.2 $(M + H)^+$; MALDI-TOF-MS *m*/*z*: 470.4 $(M + Na)^+$. UPLC-TOF-MS *m*/*z*: 448.1794 (M + H).

Antinociceptive Tests. Male Sprague−Dawley rats (Panlab) weighing 200−250 g were used. They were housed singly in a room with a controlled temperature at 21 °C on a 12 h light−dark cycle. Food and water were available ad libitum. Animals were marked for identification and allowed 18 h to recover from transport and handling. Animals were handled according to the guidelines of the European Communities Council directive of November 24, 1986 (86/609/EEC) and in all cases were treated in accordance to the Declaration of Helsinki and with The Guide for the Care and Use of Laboratory Animals as adopted and promulgated by the U.S. National Institutes of Health and the Spanish Ethical Committee. Experiments were conducted during the light phase.

Antinociception was measured using the tail flick[19] and the paw pressure[20] tests. The tail reflex was elicited by placing the tip of the rat tail over a slit through which the light of a 300 W quartz projection bulb was focused and the time to tail withdrawal was recorded. A cut-off time of 10 s was chosen to avoid tissue damage, i.e., failure to respond in 10 s resulted in termination of the test.

Mechanical nociceptive thresholds were determined by the paw pressure test on the left hind paw. Pain thresholds were measured using an analgesymeter (Ugo-Basile, Milano, Italy). The apparatus was set up to apply a force of between 0 and 1000 g, increasing from zero at a rate of 64 g/s. The nociceptive threshold was taken as the point at which the rat vocalized or struggled vigorously. Rats that did not attempt to remove their paws or vocalize before the 1000 g point was reached (when pressure exerted is 564 g/mm^2) were recorded as having reached the cut-off pressure.

In all experiments, the order of testing the animals was first paw pressure and second tail flick in order to reduce errors due to interaction between tests. All animals were tested immediately before administration of the drugs, and those rats showing control responses greater than 75% of the chosen cut-off values were discarded before further testing. Each animal served as its own control, and the percentage of antinociception was calculated as follows:

Scheme 1. Synthesis of M6Man (**2**)

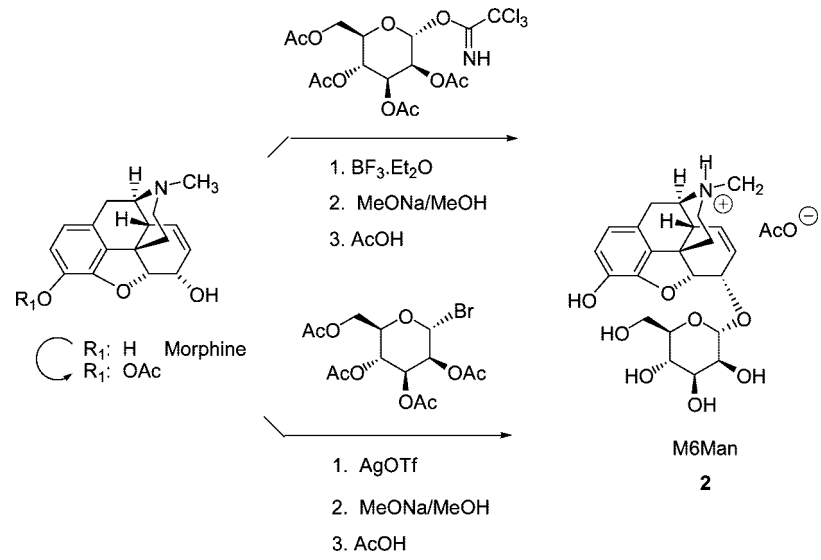

$$\%\text{MPE} = \frac{(\text{post drug score}) - (\text{control score})}{(\text{cut-off value}) - (\text{control score})}$$

Both tests were carried out with the operator being unaware of whether an animal was drug or vehicle treated. Statistical analysis of the results was assessed by the Mann−Whitney U-test.

Cardiovascular Tests. Male Sprague−Dawley rats (Panlab) were used with a weight between 250 and 300 g. The animals were housed under standard laboratory conditions of lighting and feeding.

For the surgical procedure, rats were anaesthetized with urethane (1.25 g/kg ip) and were kept at constant temperature (37 ± 0.5 °C) by a homeostatic temperature control system using a Harward thermal blanket connected to a thermostat. After the anesthesia had taken effect, the animals' tracheas were cannulated with a polyethylene cannula of 2.10 mm external diameter and this was fixed in place, allowing the animals to breathe room air spontaneously. Following this, the carotid artery and jugular vein were cannulated in order to record the variations occurring in the cardiovascular parameters and to administer the different substances at iv level. The cannula inserted into the carotid artery was connected via a Druck Prdr 75 transducer to a four-channel Lectromed recording apparatus.

After the preparatory surgical techniques had been performed, the animals were kept in response and at a constant temperature for at least one hour before starting the study protocol. Maximal arterial pressure (MAP) was kept stable at about 60 mmHg. The follow-up lasted 30 min in all cases. After the animals had become stabilized, a 0.9% saline solution was infused, followed by the dose of opioid to be studied; this was administered in physiological saline dilution in a total volume of 150−200 μL through the jugular vein over a period of 60 ± 20 s. Later, the cardiovascular variables were monitored for a 30 min period. Thus, recordings for MAP, systolic arterial pressure (SAP), diastolic arterial pressure (DAP) in mm Hg, and HR in beats per min were obtained and results were expressed as mean ± standard error of the mean of groups of 15 animals. Because the MAP and HR remained constant when physiological saline was administered, the values obtained are the means of the percent variation in the variables mentioned at each moment with respect to zero time. Values with $p < 0.05$ according to Student's *t* test were considered to be statistically significant. Means were compared by analysis of variance using the Newman−Keuls test. It had previously been ascertained that the samples had a normal distribution using the Kolmogorov−Smirnov test.

Calculation of the percentage of variation in MAP and HR was done using the following expression:

$$\%\text{variation} = \frac{(\text{post drug value}) - (\text{predrug value})}{(\text{predrug value})} \times 100$$

Statistical significance was expressed as * if $p < 0.05$, ** if $p < 0.01$, and *** if $p < 0.001$.

Tolerance Studies. Repeated doses of compound **2** (0.05, 0.1, 1, and 5 mg/kg ip, once per day for 9 consecutive days) were administered to different groups of Male Sprague−Dawley rats (Panlab) weighing between 250 and 300 g. Antinociception was measured daily 30 min after each injection of the compound by following the protocol of the tail flick test reported above.

Cell Culture and Membrane Preparation. Human embryonic kidney (HEK-293) cells stably transfected with cDNA encoding rat μ opioid receptor tagged at the N-terminal with epitope tag sequence HA were grown in T-75 cm^2 tissue culture flasks containing media (Dulbecco's modified Eagle's medium, supplemented with 10% fetal bovine serum, 100U/mL penicillin, 0.1 mg/mL streptomycin, 25 μg/mL fungizone, and 0.25 mg/mL G418) at 37 °C under a 5% CO_2 atmosphere.

Cells were grown to 80% confluence, harvested in PBS pH 7.4 containing 2 mM EDTA, and collected by centrifugation at 500*g*. Various cell pellets were resuspended in 50 mM Tris-HCl buffer pH 7.4 and homogenized in a potter homogenizer. The homogenates were centrifuged at 4100*g* for 15 min al 4 °C and the pellets washed in assay buffer, homogenized, and centrifuged twice. Membranes were resuspended in 50 mM Tris-HCl buffer pH 7.4, and the protein concentration was determined by the Lowry method (Onishi and Barr modification).

Competition Binding Assays. First 25 μg of protein were incubated with different concentrations of unlabeled morphine or morphine-6-mannoside (**2**), ranging from 0.3 nM to 10 μM and using [^{3}H]-diprenorphine (1.5 nM) as the radioligand. Then reactions were incubated at 25 °C in a final volume of 250 μL for 90 min and 10 μM naloxone was used to determine nonspecific binding. The reaction was stopped by adding 4 mL of ice-cold Tris-HCl 50 mM pH 7.4 buffer, and the mixture was rapidly filtered using a Brandel cell harvester and washed three times onto GF/B glass-fiber filters. The filters were placed in EcoScint A scintillation liquid and the radioactivity was counted using a Beckman Coulter scintillation counter. All experiments were performed in duplicate and repeated at least three times. Data were analyzed using the GraphPad Prism software, and the mean effective doses were obtained for both ligands. The inhibition constant (K_i) values were calculated using the correction of Cheng and Prusoff.[40] In all cases, data were fit to the one-site or two-site binding model and compared by using the nonlinear least-squares curve-fitting, which is based upon a statistical *F* test.

Molecular Mechanics Calculations. The relaxed (ϕ,Ψ) energy maps for compounds **1** and **2** were generated by systematic rotations around the glycoside and aglyconic bond using a grid step of 18°,

optimization of the geometry at every Φ, Ψ point using conjugate gradient iterations until the rms derivative was smaller than 0.05 kJ mol^{-1} $Å^{-1}$, and energy calculation using the MM3* force field (GB/SA solvent model for water) as integrated in the MAESTRO program. The *gg* and *gt* orientations of the lateral chain of the mannose moiety[41] of **2** were taken into account because they have been shown to be much more stable than the alternative *tg* conformer. Thus, two starting structures were considered, and in total, 800 conformers were calculated. From these relaxed energy maps, adiabatic surfaces were built by choosing the lowest energy structure for a given Φ, Ψ point. The probability distribution was calculated for each point according to a Boltzmann function at 298 K. The molecular dynamics simulations were also performed using the MM3* force field. For these simulations, several geometries, corresponding to the different low energy minima, were used as input. A temperature of simulation of 300 K was employed with a time step of 1.5 fs and an equilibration time of 100 ps, with the GB/SA solvent model for water. The total simulation time for each compound was 7 ns.

***J* and NOE Calculations.** The vicinal coupling constants were calculated for each conformation using the Karplus−Altona equation.[33] Ensemble average values were calculated from the distribution according to: $J = \sum P_{\Phi\Psi} J_{i\Phi\Psi}$. The interproton average distances were calculated using the following expression: $\langle r^{-6} \rangle_{kl} = \sum P_{\Phi\Psi} r^{-6}_{kl(\Phi\Psi)}$. To deduce the interproton distances, relaxation matrix calculations were performed using our own software, which is available upon request.[42] Isotropic motion and external relaxation of 0.1 s^{-1} was first assumed. Nevertheless, by using a single global motion rotational correlation time, it was also impossible to quantitatively fit, in a simultaneous manner, all the cross peaks belonging to the different parts of the molecules. Thus, different effective correlation times were used for the intrasugar cross peaks and for the sugar−morphine cross peaks. This is a clear indication of the internal flexibility of this molecule with distinct motion in its different parts.[37] Within the sugar ring, a correlation time of 220 ps (**1**) or 280 ps (**2**) was used to obtain the best match between experimental and calculated NOEs for the chosen intraresidue proton pair.

NMR Spectroscopy. Each molecule (ca. 5 mM) was dissolved in aqueous (D_2O) solution. NMR experiments were recorded on a Bruker Avance 500 instrument at 25 °C. Chemical shifts were referenced to external DSS in D_2O. One-dimensional spectra were acquired using 32K data points, which were zero-filled to 64K data points prior to Fourier transformation. Absolute value COSY and HMBC and phase-sensitive HSQC and HSQC-TOCSY spectra, as well as NOESY experiments (mixing times of 300, 400, and 700 ms) were acquired using standard techniques. Acquisition data matrices were defined by 2K × 256 points, multiplied by appropriate window functions and zero-filled to 2K × 512 matrices prior to Fourier transformation. Baseline correction was applied in both dimensions. Spectra were processed using the Bruker XWIN-NMR program on a personal computer.

For the experiments in SDS micelles, a 2 mM concentration of **1** or **2** was employed with a SDS concentration of 40 mM. DOSY experiments were employed to monitor integration of the morphine derivatives into the micelle. The two free ligands have analogous values for the Log of the diffusion coefficient, around −9.37, whereas, in presence of SDS, the Log *D* values significantly increased to −9.70 and −9.95 for **1** and **2**, respectively. In this case, NOESY experiments were performed with mixing times of 100, 150, and 250 ms.

Acknowledgment. This work was supported by the Fundació La Marató de TV3 (Year 2006 edition, ref 070430) and initiated with grants from CDTI (EUREKA 391 and 96 0175 to Farmhispania S.A.). Other grants from the Ministry of Education and Science of Spain (CTQ 2006 10874 CO2 01) and EC Marie Curie Research Training Network (contract no. MRTN CT 2005 019561) are gratefully acknowledged. The CAI NMR facility at the University Complutense of Madrid is thanked for data collection at the 500 MHz spectrometer. We are in debt to Isidro Liñán Castellet for coordinating many administrative and legal aspects of this study. We thank Professor Raymond A. Dwek from the Oxford Glycobiology Institute, Department of Biochemistry, University of Oxford for critically reading the manuscript and for kind advice on its publication.

Supporting Information Available: Detailed data include MM/MD calculations, supplementary NMR information data, and HPLC and MS data. This material is available free of charge via the Internet at http://pubs.acs.org.

References

(1) MacQuay, H. Opioids in pain management. *Lancet* **1999**, *353*, 2259.
(2) Corbett, A. D.; Henderson, G.; McKnight, A. T.; Paterson, S. J. 75 years of opioid research: the exciting but vain quest for the Holy Grail. *Br. J. Pharmacol.* **2006**, *147* (1), S153–162.
(3) Garber, K. Peptide leads new class of chronic pain drugs. *Nat. Biotechnol.* **2005**, *23*, 399.
(4) Hanessian, S.; Parthasarathy, S.; Maudit, M.; Payza, K. The power of visual imagery in drug design. Isopavines as a new class of morphinomimetics and their human opioid receptor binding activity. *J. Med. Chem.* **2003**, *46*, 34–48, and references cited therein.
(5) Mulder, G. J. Pharmacological effects of drug conjugates: is morphine 6-glucuronide an exception? *Trends Pharmacol. Sci.* **1992**, *13*, 302–304.
(6) Osborne, R. J.; Joel, S. P.; Trew, D.; Slevin, M. L. The analgesic activity of morphine-6-glucuronide. *Lancet* **1988**, *1*, 828.
(7) Lötsch, J.; Geisslinger, G. Morphine-6-glucuronide: an analgesic of the future? *Clin. Pharmacokinet.* **2001**, *40*, 485–499.
(8) (a) Kilpatrick, G. J.; Smith, T. W. Morphine-6-glucuronide: Actions and mechanisms. *Med. Res. Rev.* **2005**, *25*, 521–544. (b) Joshi, G. P. Morphine-6-glucuronide, an active morphine metabolite for the potential treatment of post-operative pain. *Curr. Opin. Investig. Drugs* **2008**, *9*, 786–799.
(9) The clinical trial was initiated by CeNeS Pharmaceuticals plc which has been recently acquired by PAION AG.
(10) Poeaknapo, C.; Schmidt, J.; Dräger, B.; Zenk, M. H. Endogenous formation of morphine in human cells. *Proc. Natl. Acad. Sci. U.S.A.* **2004**, *101*, 14091–14096.
(11) Boettcher, C.; Fellermeier, M.; Boettcher, C. How human neuroblastoma cells make morphine. *Proc. Natl. Acad. Sci. U.S.A.* **2005**, *102*, 8495–8500.
(12) Goumon, Y.; Muller, A.; Glattard, E. Indentification of morphine-6-glucuronide in chromaffin cell secretory granules. *J. Biol. Chem.* **2006**, *281*, 8082–8089.
(13) Glattard, E.; Muller, A.; Aunis, D.; Metz-Boutigue, M. H.; Stefano, G. B.; Goumon, Y. Rethinking the opiate system? Morphine and morphine-6-glucuronide as new endocrine and neuroendocrine mediators. *Med. Sci. Monit.* **2006**, *12*, SR25–SR27.
(14) Stachulski, A. V.; Scheinmann, F.; Ferguson, J. R.; Law, J. L.; Lumbard, K. W.; Hopkins, P.; Patel, N.; Clarke, S.; Gloyne, A.; Joel, S. P. Structure−activity relationships of some opiate glycosides. *Bioorg. Med. Chem. Lett.* **2003**, *13*, 1207–1214.
(15) Carrupt, P. A.; Testa, B.; Bechalany, A.; El Tayar, N.; Descas, P.; Perrissoud, D. Morphine-6-glucuronide and morphine-3-glucuronide as molecular chamaleons with unexpected lipophilicity. *J. Med. Chem.* **1991**, *34*, 1272–1275.
(16) Gaillard, P.; Carrupt, P. A.; Testa, B. The conformation-dependent lipophilicity of morphine glucuronides as calculated from their molecular lipophilicity potential. *Bioorg. Med. Chem. Lett.* **1994**, *4*, 737–742.
(17) (a) Toshima, K.; Tatsuka, K. Recent progress in *O*-glycosylation methods and its application to natural product synthesis. *Chem. Rev.* **1993**, *93*, 1503–1531. (b) ToshimaK.; Sasaki, K. *O*-Glycosidation Methods. In *Comprehensive Glycoscience. From Chemistry to Systems Biology*, 1st ed.; Boons, G.-J., Lee, Y. C., Suzuki, A., Taniguchi, N., Voragen, A. G. J., Eds.; Elsevier: Oxford; 2007; Vol. 1, pp 261−311.
(18) Schmidt, R. R.; Michel, J. New methods for the synthesis of glycosides and oligosaccharides. Are there alternatives to the Köenigs−Knorr method? *Angew. Chem., Int. Ed.* **1996**, *25*, 212–235.
(19) D'Amour, F. E.; Smith, D. L. A method for determining loss of pain sensations. *J.Pharmacol. Exp. Ther.* **1941**, *72*, 74–79.
(20) Randall, L. O.; Selito, J. J. A method for measurement of analgesic activity on inflamed tissue. *Arch. Int. Pharmacodyn. Ther.* **1957**, *11*, 409–419.
(21) Chaipatikul, V.; Loh, H. H.; Law, P. Y. Ligand-Selective Activation of μ-Opioid Receptor: Demostrated with Deletion and Single Amino Acid Mutations of Third Intracellular Loop Domain. *J. Pharmacol. Exp. Ther.* **2003**, *305*, 909–918.

(22) Jinsmaa, Y.; Marczak, E. D.; Balboni, G.; Salvadori, S.; Lazarus, L. H. Inhibition of the development of morphine tolerance by a potent dual mu-delta-opioid antagonist, H-Dmt-Tic-Lys-NH-CH2-Ph. *Pharmacol., Biochem. Behav.* **2008**, *90*, 651–667.
(23) Wang, Y.; Mitchell, J.; Moriyama, K.; Kim, K. J.; Sharma, M; Xie, G. X.; Palmer, P. P. Age-dependent morphine tolerance development in the rat. *Anesth. Analg.* **2005**, *100*, 1733–1739.
(24) Joharchi, K.; Jorjani, M. The role of nitric oxide in diabetes-induced changes of morphine tolerance in rats. *Eur. J. Pharmacol.* **2007**, *570*, 66–71.
(25) Thornton, S. R.; Wang, A. F.; Smith, F. L. Characterization of neonatal rat morphine tolerance and dependence. *Eur. J. Pharmacol.* **1997**, *340*, 161–167, For more information on ALZET Osmotic Pumps, see: http://www.alzet.com/. .
(26) Christrup, L. L. Morphine metabolites. *Acta Anaesthesiol. Scand.* **1997**, *41*, 116–122.
(27) For a detailed view on how the calculations were performed, see: (a) Asensio, J. L.; Martín-Pastor, M.; Jimenez-Barbero, J. The use of CVFF and CFF91 force fields in conformational analysis of carbohydrate molecules—comparison with AMBER molecular mechanics and dynamics calculations for methyl alpha-lactoside. *Int. J. Biol. Macromol.* **1995**, *17*, 137–148.
(28) Allinger, N. L.; Yuh, Y. H.; Lii, J. H. Molecular mechanics. The MM3 force field for hydrocarbons. 1. *J. Am. Chem. Soc.* **1989**, *111*, 8551–8566.
(29) Mohamadi, F.; Richards, N. G. J.; Guida, W. C.; Liskamp, R.; Lipton, M.; Caufield, C.; Chang, G.; Hendrickson, T.; Still, W. C. *J. Comput. Chem.* **1990**, *11*, 440–467.
(30) For the application of molecular mechanics force fields to the conformational analysis of carbohydrate molecules, see (a) Pérez, S.; Imberty, A.; Engelsen, S.; Gruza, J.; Mazeau, K.; Jiménez-Barbero, J. Poveda, A.; Espinosa, J. F.; van Eyck, B. P.; JohnsonG., et al. *Carbohydr. Res.* **1998**, *314*, 141−155.
(31) For a survey of NMR methods and data applied to saccharide molecules, *NMR Spectroscopy of Glycoconjugates*; Jiménez-Barbero, J., Peters, T., Eds.; Wiley-VCH: Weinheim, 2002.
(32) See: *Anomeric Effect. Origin and Consequences.* ; ACS Symposium Series 87; Szarek, W. A., Horton, D., Eds.; American Chemical Society: Washington, D. C., 1979.
(33) Gylbert, L. The crystal and molecule structure of morphine hydrochloride trihydrate. *Acta Crystallogr., Sect. B: Struct. Sci.* **1973**, *29*, 1630–1635.
(34) Haasnoot, C. A. G.; de Leeuw, F. A. A. M.; Altona, C. The relationship between proton−proton NMR coupling constants and substituent electronegativities, I. *Tetrahedron* **1980**, *36*, 2783–2792.
(35) Espinosa, J. F.; Bruix, M.; Jarreton, O.; Skrydstrup, T.; Beau, J.-M.; Jiménez-Barbero, J. Conformational differences between *C*- and *O*-glycosides: The α-*C*-mannobiose/α-*O*-mannobiose case. *Chem.—Eur. J.* **1999**, *5*, 442–448.
(36) Neuhaus, D.; Williamson, M. P. The Nuclear Overhauser Effect. In *Structural and Conformational Analysis*; VCH: New York, 1989.
(37) Poveda, A.; Asensio, J. L.; Martín-Pastor, M.; Jimenez-Barbero, J. Solution conformation and dynamics of a tetrasaccharide related to the Lewis(x) antigen deduced by NMR relaxation measurements. *J. Biomol. NMR* **1997**, *10*, 29–43.
(38) See, for instance, *Computer Modelling of Carbohydrate Molecules*, ; ACS Symposium Series 430; French, A. D., Brady, J. W., Eds.; American Chemical Society: Washington DC, 1990.
(39) See, for instance,(a) Martin-Pastor, M.; Espinosa, J. F.; Asensio, J. L.; Jimenez-Barbero, J. A comparison of the geometry and of the energy results obtained by application of different molecular mechanics force fields to methyl α-lactoside and the C-analogue of lactose. *Carbohydr. Res.* **1997**, *298*, 15–49.
(40) Cheng, Y. C.; Prusoff, W. H. Relationship between the inhibition constant (K_i) and the concentration of inhibitor which causes 50% inhibition (IC_{50}) of an enzymatic reaction. *Biochem. Pharmacol.* **1973**, *22*, 3099–3108.
(41) For instance, (a) Asensio, J. L.; Cañada, F. J.; Kahn, N.; Mootoo, D. A.; Jiménez-Barbero, J. Conformational differences between *O*- and *C*-glycosides: the α-*O*-man-(1→1)-beta-Gal/alpha-C-Man-(1→1)-beta-Gal case—a decisive demonstration of the importance of the *exo*-anomeric effect on the conformation of glycosides. *Chem.—Eur. J.* **2000**, *6*, 1035–1041.
(42) Asensio, J. L.; Cañada, F. J.; Garcia-Herrero, A.; Murillo, M. T.; Fernández-Mayoralas, A.; Johns, B. A.; Kozak, J.; Zhu, Z. Z.; Johnson, C. R.; Jiménez-Barbero, J. Conformational Behavior of Aza-*C*-Glycosides: Experimental Demonstration of the Relative Role of the *exo*-Anomeric Effect and 1,3-Type Interactions in Controlling the Conformation of Regular Glycosides. *J. Am. Chem. Soc.* **1999**, *121*, 11318–11329.

JM8011245